Research Square

Preprints are preliminary reports that have not undergone peer review.
They should not be considered conclusive, used to inform clinical practice,
or referenced by the media as validated information.

Universal approach to in situ light-coupled NMR spectroscopy without fibre optics

Jack Bramham
The University of Manchester https://orcid.org/0000-0002-2793-6883
Alexander Golovanov (A.Golovanov@manchester.ac.uk)
The University of Manchester https://orcid.org/0000-0002-8592-3984

Article

Keywords:

Posted Date: December 3rd, 2021

DOI: https://doi.org/10.21203/rs.3.rs-1131472/v1

License: This work is licensed under a Creative Commons Attribution 4.0 International License.
Read Full License

Version of Record: A version of this preprint was published at Communications Chemistry on August 4th, 2022. See the published version at https://doi.org/10.1038/s42004-022-00704-5.

Abstract

In situ illumination of liquid-state nuclear magnetic resonance (NMR) samples makes it possible for a wide range of light-dependent chemical and biological phenomena to be studied by the powerful analytical technique. However, the position of an NMR sample deep within the bore of the spectrometer magnet renders such illumination challenging. Here, we demonstrate a photo-NMR insert device (NMRtorch) where a lighthead containing an LED array is attached directly to the top of an NMRtorch tube. The wall of the tube itself acts as a light guide, illuminating the sample from the outside. We explore how this new setup performs in a number of photo-NMR applications, including photoisomerisation and photo-chemically induced dynamic nuclear polarisation (photo-CIDNP), and demonstrate the potential for ultraviolet (UV) degradation studies with continuous online NMR assessment. This setup enables users of any typical liquid-state spectrometer to easily perform *in situ* photo-NMR experiments, using a wide range of wavelengths.

Introduction

Light is a form of electromagnetic energy that surrounds and affects life on earth, with a myriad of chemical and biological reactions dependent upon light. Ultraviolet (UV), visible, and infrared (IR) light can also act as ideal triggers to connect our macroscopic world with the nanoscale or molecular world, for example, to modulate material properties[1,2], molecular switches[3], gene expression[4], targeted drug release[5,6], enzymatic reactions[7–9], and many other physical processes. The ability to incorporate controlled light illumination into experimental and analytical procedures is therefore essential.

Nuclear magnetic resonance (NMR) spectroscopy is one of the most powerful and universal analytical techniques, and is used widely throughout science to study the properties and behaviour of molecules, reactions and materials.[10] Given the capabilities of NMR spectroscopy, a number of approaches to illuminate NMR samples have been developed (recently comprehensively reviewed by Nitschke, et al. [11] and Ji, et al. [12]), allowing a number of light sensitive systems, including photocatalysed reactions[13,14] and polymerisation,[15,16] to be studied by light-coupled NMR spectroscopy (often referred to as simply photo-NMR). Furthermore, illumination may be directly beneficial for some NMR applications; for example, by dramatically improving signal intensity through photo-chemically induced nuclear polarisation (photo-CIDNP), enabling the detection of nanomolar quantities of biomolecules,[17–20] or allowing studies of proteins[21–23] or chemical reactions.[24]

Direct *in situ* illumination of samples inside the NMR spectrometer, coinciding with spectral acquisition, is largely preferable to *ex situ* illumination.[11] However, the position of an NMR sample deep within the magnet bore of a typical NMR spectrometer makes it technically challenging to deliver sufficient levels of light to uniformly illuminate the sample. Historically, external LASERs guided by mirrors, glass rods or optical fibres have been used,[25–27] but such light sources are relatively expensive and prone to intense localised sample heating, with a fairly limited variety of wavelengths usually available in a specific lab.[11]

Furthermore, open-beam systems with mirrors may require complex adjustments and additional safety measures, while systems using optical fibres may suffer from losses of light.[28] Moreover, such fibres and associated inserts may hinder magnetic field homogeneity, and can be generally difficult to work with, leading to low sample throughput. Recently, the rapid development and availability of inexpensive and powerful light emitting diodes (LEDs) with a wide choice of emission wavelengths has led to their increasing use as light sources in photo-NMR.[12,13,29–32] Although NMR probe modifications to incorporate LED illumination directly inside the probehead have been suggested,[26,33] optical fibres (either alone or inside a coaxial insert) are still typically used to guide light from the LED positioned outside the NMR spectrometer to the NMR sample inside the magnet. However, these setups also suffer from the same disadvantages inherent to the LASER-fibre optic system, with the additional difficulty of coupling poorly collimated light from an LED into a thin optical fibre, leading to significant light intensity losses.[12,29]

In this work, we introduce an alternative universal strategy for delivering light generated by LEDs to typical solution-state NMR samples, without the need for fibre optics, or probehead modifications. In our design (which we named 'NMRtorch'), one or more LEDs are mounted in a lighthead attached directly to the top of an NMRtorch tube, with this assembly inserted into the NMR magnet bore. The wall of the tube itself acts as a light guide, with light scattered only around the sample volume by special etchings covering this area, resulting in uniform illumination from the *outside* of the sample.

Here, we demonstrate the potential and capability of this new *in situ* photo-NMR approach to study a wide variety of phenomena. Firstly, we demonstrate very significant signal enhancements obtained in photo-CIDNP experiments, and show how light uniformity and intensity inside the NMR samples can be assessed, and optimised through positioning of light scattering etchings. We show that several LEDs of different colours can be used in the same experiment, with complete NMR spectrometer control alongside RF pulses, e.g., to study kinetics of photoreactions. We also show that our approach enables the delivery of significant UV radiation dosage within a short period of time, thus making photostability studies of chemicals and pharmaceuticals with simultaneous NMR detection possible. The convenience of using these design principles is expected to make photo-NMR applications more accessible on a wide range of old and new NMR spectrometers and probeheads.

Materials And Methods

NMRtorch apparatus

The NMRtorch insert apparatus consists of: (i) a special light-conducting NMR sample tube; (ii) a lighthead which houses LEDs, positions them at the top of the NMRtorch tube and provides cooling for them; (iii) a power supply module; and (iv) connecting electric cables. Non-magnetic LEDs or LED arrays from different manufacturers were employed here, showing marginal difference in performance, with nominal emission wavelength and power as indicated below for specific applications. A range of one- and four-channel power supplies to drive LEDs at constant currents, as per individual LED specifications,

with transistor-transistor logic (TTL) trigger controls, were assembled in-house, as well as a number of lightheads with different combinations of LEDs. Heavy-walled 5 mm borosilicate (Wilmad/Hilgenberg) and quartz glass (Norell) NMR tubes were adapted by etching patterns on the exterior surface of the tubes around the bottom 40-42 mm area where the standard-size sample is located, thus making NMRtorch tubes. A range of transparent and semi-transparent tube caps from different materials were trialled, however we did not find the characteristics of this component critical for the experiments, as long as the cap tolerated local heating from the LED.

NMR Spectroscopy

NMR experiments were performed on a Bruker 500 MHz Avance III spectrometer using a QCI-F cryoprobe with cooled ^{1}H and ^{19}F channels and sample temperature control unit. Spectra were initially processed and analysed using Topspin 4.1 and Dynamics Center 2.7 (both Bruker), and plotted in GraphPad Prism 9.

Photo-CIDNP

6-fluoroindole (6FI, Fluorochem) was prepared as a 250 mM stock solution in deuterated dimethylsulfoxide (99.8% DMSO-d6, Eurisotop), and diluted as required with H_2O and 10% $^{2}H_2O$ (Sigma-Aldrich). Riboflavin 5'-monophosphate sodium salt hydrate (FMN, Sigma-Aldrich) was prepared as concentrated 10 mM stock, and added to the final samples immediately before experiments. No attempts were made to degas samples, or remove oxygen. The samples were placed in NMRtorch tubes and sealed with the transparent caps. The photo-CIDNP enhancement factor α has been calculated as:

$$\alpha = \frac{\left| I_L \right|}{I_D} \quad \text{(Equation 1)}$$

where I_L and I_D is the signal intensities in the illuminated and in the dark state, respectively. Light intensity (photosynthetic photon flux density, PPFD) at the exterior surface of the tube just outside the sample volume was measured with a calibrated Li-250A photometer and Li-190R quantum sensor (both Li-Cor).

Measuring Of Light Distribution In NMRtorch Tubes

Pixel brightness images of selected example NMRtorch tubes with different patterns and degrees of etching were captured with a Pixel 4A (Google), and analysed for greyscale values in ImageJ software. Saturated fluorescein (Fluka) solution was prepared in water. Photo-CIDNP NMR imaging experiments were acquired with standard *zg* pulse sequence with ^{19}F detection, modified to include variable light illumination before the 90° pulse, and application of a 0.106 G cm^{-1} magnetic field gradient (G_z) during FID acquisition, typically with 4 scans. Dark spectra were recorded with the same pulse sequence

beforehand without illumination with a sufficient number of scans (typically 16) to obtain the reference imaging profile for a given sample. In these imaging experiments, signals are offset in frequency (Ω) according to:

$$\Omega = \gamma G_Z Z \quad \text{(Equation 2)}$$

where γ is gyromagnetic ratio, and Z is vertical position relative to the coil centre. To examine light distribution along the vertical Z axis of the sample and remove the effect of gradient non-linearity at the edges, enhancement factors (α_Z) at each point in the imaging spectra were calculated and related to the vertical position Z in the sample:

$$\alpha_Z = \frac{\left| I_L^\Omega \right|}{I_D^\Omega} \quad \text{(Equation 3)}$$

where I_L^Ω and I_D^Ω are profile intensities (normalised by the number of scans) in the illuminated and reference dark spectra at frequency offset Ω, respectively. The values of α_Z were used as a measure of local light intensity across the NMR-observable area of the sample.

Azobenzene Photoisomerisation

1 mM 4-aminoazobenzene (AAB, Fluorochem) was prepared in deuterated dimethylsulfoxide (99.8% DMSO-d6, Eurisotop). *In situ* NMR light illumination was performed with a lighthead containing red, green, blue and white LED array driven at 3W (0.7A current) per colour channel. As sample preparation under ambient light may lead to a poorly defined initial isomerisation state, the sample was pre-equilibrated *in situ* with blue light for 5 minutes before the start of acquisition. ^{1}H NMR kinetic experiments were recorded at 5 s intervals with a pseudo-2D *zgesgp* pulse sequence, with 1 scan and 0 dummy scans, with the initial four spectra acquired in the series discarded to allow for magnetisation equilibration.

Quinine Photodegradation

2% (w/v) quinine hydrochloride dihydrate (Sigma-Aldrich) was prepared fresh as required in Milli-Q water with 10% ^2H_2O (Sigma-Aldrich). Quinine is the standard calibration material for UV photostability testing, as per International Council for Harmonisation of Technical Requirements for Pharmaceuticals for Human Use (ICH) Q1B guidelines.[34,35] *In situ* illumination was performed with a UV LED array (nominal 365 nm peak emission, 10 W power), in NMRtorch tubes made of either borosilicate glass or quartz. UV-Vis spectra for control (foil-wrapped to protect from light and stored at the same temperature for the duration of the experiment) and illuminated samples were recorded using a Nanodrop 2000 (ThermoScientific).

Results

Principles of the NMRtorch design

In our proposed approach to illuminating NMR samples *in situ*, a lighthead (Figure 1) containing one or more LEDs is attached directly to the top of an NMRtorch tube, allowing light to enter the walls of the glass tube through the rim. If used, the tube cap should be sufficiently optically clear (Figure 1A). Optional optical elements, such as lenses or condensers, may be used to further focus light, although we found these to be of little benefit given the close proximity of the LED emitter to the top rim of the tube. The NMR tube itself acts as a light guide, with light confined within the optically-transparent wall of the tube, and propagated towards the sample area (standard borosilicate or quartz 5 mm tubes with ~1.4 mm wall thickness work well in our experience). In NMRtorch tubes, the glass around the sample volume at the bottom of the tube is modified by the introduction of light scattering centres (achieved here by etching of the exterior surface). When the LEDs are illuminated, light is scattered here, thus preferentially illuminating the sample area from the *outside* (Figure 1A).

The lighthead is connected by a multicore electrical cable to an electrical control box containing constant-current power supplies, with their triggers in turn connected to the NMR console controlled by a computer (Figure 1B). Furthermore, in the NMRtorch setup described here, four separate channels connect to the NMR console, allowing the use of multi-channel LED arrays, to maximize light output at a single wavelength, or to provide illumination at different wavelengths. In the current implementation, the NMR tube and attached lighthead are manually lowered into the spectrometer bore by the multicore electrical cable. Gas flow that is typically present in the magnet bore provides sufficient cooling for LEDs with lower power consumption (≤3W) or under operation at lower duty cycles. However, for more powerful LED arrays at constant illumination, a supplementary compressed gas line to the lighthead provides additional cooling, with temperature monitored by an optional temperature sensor in the lighthead. The proposed arrangement enables convenient delivery of high-intensity light (Figure 1C) to the sample area achieving high uniformity (Figure 1D), while essentially allowing the user to handle the NMR sample tube as normal, with easy tube filling and capping, avoiding any inserts or additional sources of magnetic field inhomogeneity in the sample area. The etchings on the outside surface of NMRtorch tubes, in our experience, do not affect NMR tuning, shimming, or water suppression, and no significant effects on the signal lineshape were observed. Furthermore, as all electrical components in the lighthead are positioned sufficiently far away from the NMR detection region, we have not noticed any signs of electromagnetic interference caused by LED switching.

Using NMRtorch For Photo-CIDNP Experiments

Photo-chemically induced dynamic nuclear polarization (photo-CIDNP), where observed NMR signal intensities of aromatic compounds in the presence of a photosensitiser are modulated upon illumination, has been previously demonstrated using illumination with LASERs,[18,20,21,36] and more recently, with

LEDs.[13,31,32] Here, we explored the suitability and effectiveness of NMRtorch for the photo-CIDNP experiments, by recording ^{19}F NMR spectra of 6-fluoroindole (6FI) with photosensitization by flavin mononucleotide (FMN) under blue light illumination. With the NMRtorch setup, 6FI exhibited emissive photo-CIDNP, with negative ^{19}F peaks upon illumination and a maximum 64-fold enhancement achieved with the lighthead containing a single LED with nominal 470 nm peak emission, 3W power consumption (Figure 2A). To our knowledge, this enhancement is the largest ever reported for ^{19}F, which is remarkable given that no attempts were made here to remove oxygen from the samples, or introduce any other measures to prevent dye quenching. Convenient working with multiple samples allowed us to explore the concentration-dependence of photo-CIDNP effects. At 0.2 mM FMN, the highest photo-CIDNP enhancements (α, Equation 1) were observed at 1 mM 6FI, with lower enhancements observed at both higher and lower concentrations (Figure 2B). As the highest absolute signal intensity for illuminated samples was observed at 6 mM 6FI (Figure 2B), this concentration was chosen for further NMR imaging experiments where absolute signal intensity is critical. Photo-CIDNP enhancements were also observed to increase with illumination time, yet began to plateau at values above 6 s (Figure 2C). We found that the easy process of sample tube filling, capping and attaching to the NMRtorch lighthead enabled multiple photo-CIDNP samples to be run efficiently and consistently.

As light intensity is an important experimental parameter, it needs to be controlled and measured in the sample area. LED brightness can be routinely dimmed by controlling duty cycle through pulse width modulation (PWM). Here, we incorporated this PWM control into the NMR pulse sequence, such that light intensity (between 0 and 100% duty cycle) before RF pulses was controlled directly by the NMR console (see Supplemental Appendix S1). Both the ^{19}F NMR photo-CIDNP effect for 6FI, and the light intensity measured *ex situ* on the surface of the sample area, were observed to be linear with LED duty cycle (Figure 2D). This linearity of 6FI photo-CIDNP effect with increasing light intensity means this parameter can be used to assess the uniformity of light distribution across the length of the NMR sample in 'NMR imaging' experiments. Although photo-CIDNP has previously been used to assess the effectiveness of sample illumination approaches[29] and light distribution uniformity,[28] here, to account for non-linearity of magnetic field gradients et the edges of NMR-active volume, we propose to use position-dependant photo-CIDNP enhancement factors, rather than a raw photo-CIDNP spectra [28] obtained in imaging experiments. As the photo-CIDNP signal intensities and enhancement factors are directly proportional to the light intensity, the profiles formed by position-dependent enhancement factors (α_Z, defined by Equation 3) report directly on light intensity distribution inside the sample, along Z-axis.

In the NMRtorch setup, the positioning of light scattering centres (created here by etchings on the outside surface of the tube) controls light distribution and intensity (Figure 3). Excessive etchings at the top of the sample may cause the majority of light to be scattered at the top, with less light reaching the bottom of the sample area. We therefore propose that etchings should be distributed non-uniformly across the sample length, to achieve more uniform light distribution. To demonstrate the effect of such positioning of etchings, light distribution in an illustrative set of NMRtorch tubes was assessed by both pixel brightness analysis of photo images, and photo-CIDNP position-dependent enhancement factors α_Z.

Here, smoothed pixel brightness characterisations of light distribution (Figure 3B, with ± 2.5 mm moving averages) were in good agreement with the observed photo-CIDNP position-dependent enhancements across the NMR-active volume (Figure 3C). In the control unetched Tube 1, scattering was primarily observed at the sample meniscus and tube bottom, resulting in poor sample illumination and weak photo-CIDNP effects. Conversely, in sample tubes with various etched patterns (Tubes 2 – 4), light scattering results in greater sample illumination and thus greater position-dependent signal enhancement (α_Z). This distribution of etchings can be used to guide light distribution in the sample: for example, in Tube 2, the etched bottom portion experiences greater sample illumination than the unetched top portion of the sample region, whereas adding etchings in this area, in Tubes 3 and 4, increased illumination in the upper portion. Additionally, the degree of etching can be used to control overall illumination intensity, with the more frequent etchings on Tube 4 resulting in greater light intensity (averaging 260.9 ± 44.9 μmol m^{-2} s^{-1} across the sample area) and photo-CIDNP enhancements than Tube 3 (117.2 ± 33.3 μmol m^{-2} s^{-1}). Notably, in the illustrative Tubes 2-4 shown here, light was more intense at the bottom of the sample, further away from the LED, where the etchings were denser. These experiments show that by controlling the positioning of the etchings it is possible to control the light distribution around the sample area of the NMRtorch tube, with the position-dependent photo-CIDNP signal enhancement parameter α_Z being a convenient indicator of both the uniformity and overall light intensity in the sample area.

Studying Chemical Photostability Under UV Illumination

We next tested whether the NMRtorch setup could deliver high-intensity UV light to the NMR sample. Studies of photoreactions, or photodegradation of pharmaceutical and biopharmaceutical products, would both benefit from simultaneous online observation of changes in NMR spectra under very intense light. The irradiation dosage typically required for stability testing of pharmaceutical products is defined in the International Council for Harmonisation of Technical Requirements for Pharmaceuticals for Human Use (ICH) Guidelines Q1B,[34,35] and suggests the use of 2% (w/v) quinine hydrochloride as an actinometric system, with prescribed dosage corresponding to greater than 0.5 increase in light absorbance at 400 nm following the UV-A exposure. In practice, such dosage is typically achieved after several hours in specialist UV illumination chambers, which do not allow easy online monitoring of the photodegradation process.

Here, we explored whether the NMRtorch setup can deliver such a UV dosage within reasonable timeframe while allowing to monitor sample degradation by ^{1}H NMR spectra. A specialised lighthead was employed housing a 10 W UV LED array (365 nm peak wavelength), and the degradation of quinine hydrochloride was simultaneously monitored. Even when a borosilicate glass tube was used, NMR spectral changes were readily observed within minutes (Figure 4 and Supplemental Fig. S1), with change in optical density at 400 nm reaching 0.74 ± 0.02 after only 2 hours irradiation (Figure 4B), in line with ICH Q1B guidelines. Using a quartz tube instead of a borosilicate one enhanced the degradation rate by around three-fold (Supplemental Fig. S2). In the ^{1}H NMR spectra acquired during UV irradiation of

quinine, a series of phenomena were observed. Firstly, the intensity of the intact quinine peaks decreased (Figure 4C) over time, with this occurring over two distinct timescales, and the greatest changes happening over the first 20 min (Figure 4E). Monitoring signal reduction from different chemical moieties of the molecule allows to assess site-specific rates of degradation, with the quinoline moiety exhibiting greater reductions in signal intensity than the quinuclidine moiety. Secondly, significant spectral broadening was observed, particularly in the aliphatic region (Figure 4D). Finally, a number of additional spectral peaks appear, with this occurring on a similar timescale to the reductions in the intact quinine peaks (Figure 4D,F). Therefore, NMRtorch setup enables high-intensity irradiation of NMR samples *in situ* with UV light, achieving the doses prescribed by the regulatory guidelines within 2 hours of experimental time, while allowing live monitoring of photodegradation.

Studying Multi-colour Triggering Of Photoswitches

Photo-NMR may also be used to study reactions or transitions triggered by various colours of light, and is particularly well suited to studying the kinetics of such processes. The *trans-cis* isomerisation of azobenzene and its derivatives is one such light induced transition, which may serve as a useful photoswitch in biotechnology applications.[37] Although some transitions in such system have been characterised by NMR before with *in situ* illumination,[38–41], exploring transitions triggered by toggling between numerous illumination colours would be more informative. To illustrate the application of the NMRtorch approach to characterise the kinetics of photoswitches, the photoisomerisation of 1 mM 4-aminoazobenzene (AAB) in DMSO-d6 was studied under continuous illumination with a variety of light wavelengths (Figure 5). At equilibrium under darkness (Figure 5B), AAB exists entirely as the *trans* isomer. However, if the solution is illuminated with short-wavelength light, such as blue, then isomerisation occurs, shifting equilibrium towards the *cis* isomer state, giving rise to distinct upfield NMR signals (Figure 5B, marked with asterisks). Therefore, the ratio of these distinct signals can be used to derive populations of *trans* and *cis* isomers present in the sample, and track the kinetics of photoisomerisation in response to illumination by different light colours (Figure 5C). Toggling between the colours is easily achieved using a multichannel NMRtorch lighthead containing four different (RGBW) LEDs.

The light toggling experiments reveal that, irrespective to the initial equilibrium state, *trans* → *cis* isomerisation triggered by blue light is fast, with rate constant k=65 ± 6 μM min^{-1}. Illumination with each colour establishes its own characteristic *trans* – *cis* equilibrium. After blue light illumination, re-equilibration towards *trans* is faster with green light (108 ± 3 μM min^{-1}) than with red (k=93.0 ± 0.1 μM min^{-1}), but much higher equilibrium population of *trans* is reached with the red light than with the green. *Cis* → *trans* photoisomerisation under green and white light (111 ± 5 μM min^{-1}) occurs at similar rates, but result in different ultimate equilibria, with more *trans* isomer present under green light. It should be noted that in this LED white light is generated by exciting luminophore with blue light, and therefore a strong blue component in this white light is expected. Interestingly, unlike the colour-driven transitions which here all show mono-exponential behaviours, the thermal transition under darkness from *cis* to *trans*

can be only satisfactory fitted as the sum of two exponents (k_{fast}=17.9 ± 0.9 μM min^{-1}, k_{slow} = 3.5 ± 0.1 μM min^{-1}), highlighting the hidden complexity of this process uncovered by *in situ* photo-NMR experiments performed using NMRtorch. To our knowledge, the multi-stage mechanism of thermal transition under darkness for AAB has not been described before. One can also easily explore how the combination of colours would affect both the isomerisation rate and equilibrium state, and thus comprehensively characterise the behaviour of photoswitchable systems in response to different combinations of light stimuli and their intensities. The experiments here demonstrate the convenience of using NMRtorch and the potential of the multi-wavelength illumination approach in studying the kinetics of photoswitches, as well as other photo-induced phenomena which can be detected and monitored in real time by NMR spectral changes.

Discussion

In situ illumination of samples opens up a realm of potential light-sensitive experimental systems which may be studied by high-resolution NMR spectroscopy, one of the most powerful analytical techniques. Although a range of illumination strategies have been previously suggested, including guiding external light sources with optical fibres,[28,29,42] or modifying the NMR probe itself,[26,33] these solutions are generally cumbersome to use at higher throughputs, or require customised probes. Here, we present a new universal and convenient approach to illuminating NMR samples *in situ* with the LED-based NMRtorch device, which should be compatible with any typical NMR probehead, including cryoprobes. The lack of optical fibres minimises light losses and removes sources of magnetic field inhomogeneity, while allowing sample tube filling and capping to be done in the conventional manner, making photo-NMR experiments more user friendly and allowing higher throughput. One can envisage that the proposed principles can be used in automation.

In the NMRtorch approach, the lighthead containing LEDs is attached directly at the top of a special NMR sample tube, and together they are inserted into the spectrometer, enabling illumination at a wide range of wavelengths, including UV, with a minimal light transmission path length. The NMRtorch tube itself acts as a light guide, with etched patterns resulting in preferential illumination of the sample volume from the outside. Here, the position and extent of the etching used to introduce the light scattering centres was observed to have a dramatic effect on the uniformity of light distribution and the resulting photo-CIDNP NMR signal (Figure 3), in agreement with previous observations of the effect of roughening the exposed tip of fibre optics.[28,29] In our experience, both borosilicate and quartz NMRtorch tubes work well, although quartz tubes may be preferable at shorter wavelengths such as UV. As the typical light-emitting area of LEDs is comparable with the area of the transparent rim of the heavy-walled 5 mm NMRtorch sample tube, and the LEDs are in extremely close proximity to the rim, light coupling efficiency is very high, even in the absence of additional optical elements such as condenser lenses. Local heating of this coupling area is not propagated to the sample area, and any local weak electromagnetic fields associated with LED switching are largely contained inside the shielded lighthead, also distanced from the NMR

probehead. NMRtorch lightheads are generally cooled by the gas flow typically present in the magnet bore, and for more powerful LEDs, can be cooled further by the auxiliary compressed gas line.

In our experience NMRtorch did not interfere with performance of the NMR spectrometer, with no noticeable effects on the lineshape, probe tuning or shimming, or solvent suppression. No additional re-equilibration delays were needed after light switching before the start of acquisition. NMRtorch sample tubes can be filled and sealed with caps as usual, allowing to work with oxygen- or moisture-sensitive samples. Transparent or semi-transparent tube caps are required to allow enough light to enter into the rim of the tube. As the walls of the tube need to be sufficiently thick for effective propagation of light and to achieve uniform light scattering around the sample volume, the sample volume is therefore decreased to approximately 0.2 mL for 5 mm tube, which is roughly equivalent to a standard 3 mm NMR tube. As the sample volume is illuminated effectively all round from the *outside* through the glass wall, NMRtorch enables experiments with optically dense liquid samples or suspensions, with effective optical path through the sample of less than ~1.2 mm. Importantly, no other materials, except the glass sample tube and the sample, are present in the proximity of the detection area, ensuring that magnetic field homogeneity is only limited by the quality of the glass tube and the sample itself. Importantly, NMRtorch setup is expected to be compatible with any standard high-field, low-field or benchtop NMR spectrometer, or probehead, and can be adapted to suit tubes of different diameters as well.

Here, the NMRtorch demonstrated effective performance in typical photo-NMR experiments, including photo-CIDNP, studies of aminoazobenzene (AAB) photoisomerisation, and UV-induced chemical conversion. The 64-fold CIDNP enhancement observed here for 6FI with just one 3W 470 nm LED is, to our knowledge, the highest observed in ^{19}F NMR spectroscopy, either with LEDs or LASERs. This molecule, 6FI, has not been previously described as photo-CIDNP active, and its properties are well suited for assessment of light intensity distribution inside the samples, given that such enhancement is observed in the absence of any measures to remove oxygen or prevent dye quenching in the samples. For photo-CIDNP studies, we found LED pulse width modulation (PWM) control directly by the NMR console to be particularly useful and convenient, and it removes the need for additional PWM light dimming electronic components as used elsewhere.[41] The multiple channel/LED aspect of the NMRtorch approach is also particularly advantageous for studies of photoswitches. For example, although photo-isomerisation of azobenzene-based dyes has previously been studied by NMR spectroscopy using both *in*[38–41] and *ex situ*[43] illumination, rapid multicolour switching of LED illumination demonstrated here enables additional kinetic and equilibria processes to be easily observed at a number of wavelengths, reducing the dead time of the experiments, and allowing to characterise fully the behaviour of a photoswitch in response to a range of stimuli (Figure 5). Here, previously non-described bi-exponential thermal *cis*→t*rans* relaxation process of AAB in darkness have been revealed, suggesting a two-step relaxation mechanism, whereas all the light-induced transitions were mono-exponential. Finally, the NMRtorch also enables the use of very powerful LED arrays for sample illumination. Thus photodegradation studies, normally conducted in dedicated UV illumination chambers, can be combined with online NMR spectral monitoring and analysis (Figure 4). As critical light-conducting components of

NMRtorch are made of glass, with relatively large cross-sectional area, no local degradation (e.g. yellowing) of these is expected following prolonged UV exposure.

In conclusion, the modular NMRtorch approach is capable of supporting combinations of multiple LEDs with different wavelengths, with detection using any NMR pulse sequence where the light control (i.e., duration and intensity) commands can be added. As more powerful LEDs, laser diodes, or similar-sized new sources of illumination become available,[44] NMRtorch lightheads should be able to accommodate these and use for ever-increasing range of photo-NMR applications. NMRtorch can be used on all typical existing spectrometers, opening new avenues of research in light-dependent phenomena by one of the most powerful analytical techniques.

Declarations

Acknowledgements: The project supported by EPSRC New Horizons EP/V04835X/1. We acknowledge the use of the Manchester Biomolecular NMR Facility, and the assistance of the University of Manchester Mechanical Workshop. We are grateful to Matthew Cliff for help with NMR setup, and to Dimitri Golovanov for assistance with 3D computer-aided design and 3D printing.

Conflict of Interest Statement: APG is the named author in patent applications GB2008825.8 and PCT/GB2021/051254.

References

1. Gemayel, M. E. *et al.* Optically switchable transistors by simple incorporation of photochromic systems into small-molecule semiconducting matrices. *Nat Commun* **6**, 6330, doi:10.1038/ncomms7330 (2015).
2. Shanmugam, S., Xu, J. & Boyer, C. Photocontrolled Living Polymerization Systems with Reversible Deactivations through Electron and Energy Transfer. *Macromol Rapid Commun* **38**, doi:10.1002/marc.201700143 (2017).
3. Hoorens, M. W. H. *et al.* Iminothioindoxyl as a molecular photoswitch with 100 nm band separation in the visible range. *Nat Commun* **10**, 2390, doi:10.1038/s41467-019-10251-8 (2019).
4. Yamada, M., Nagasaki, S. C., Ozawa, T. & Imayoshi, I. Light-mediated control of Gene expression in mammalian cells. *Neurosci Res* **152**, 66–77, doi:10.1016/j.neures.2019.12.018 (2020).
5. Sun, C. Y., Zhang, B. B. & Zhou, J. Y. Light-activated drug release from a hyaluronic acid targeted nanoconjugate for cancer therapy. *J Mater Chem B* **7**, 4843–4853, doi:10.1039/c9tb01115c (2019).
6. Rapp, T. L. & DeForest, C. A. Targeting drug delivery with light: A highly focused approach. *Adv Drug Deliv Rev* **171**, 94–107, doi:10.1016/j.addr.2021.01.009 (2021).
7. Biegasiewicz, K. F. *et al.* Photoexcitation of flavoenzymes enables a stereoselective radical cyclization. *Science* **364**, 1166–1169, doi:10.1126/science.aaw1143 (2019).

8. Seel, C. J. & Gulder, T. Biocatalysis Fueled by Light: On the Versatile Combination of Photocatalysis and Enzymes. *Chembiochem* **20**, 1871–1897, doi:10.1002/cbic.201800806 (2019).
9. Feyza Ozgen, F. *et al.* Artificial Light-Harvesting Complexes Enable Rieske Oxygenase Catalyzed Hydroxylations in Non-Photosynthetic cells. *Angew Chem Int Ed Engl* **59**, 3982–3987, doi:10.1002/anie.201914519 (2020).
10. Keeler, J. *Understanding NMR spectroscopy*. 2nd edn, (John Wiley and Sons, 2010).
11. Nitschke, P., Lokesh, N. & Gschwind, R. M. Combination of illumination and high resolution NMR spectroscopy: Key features and practical aspects, photochemical applications, and new concepts. *Prog Nucl Magn Reson Spectrosc* **114-115**, 86–134, doi:10.1016/j.pnmrs.2019.06.001 (2019).
12. Ji, Y. *et al.* LED-Illuminated NMR Spectroscopy: A Practical Tool for Mechanistic Studies of Photochemical Reactions. *ChemPhotoChem* **3**, 984–992, doi:10.1002/cptc.201900109 (2019).
13. Feldmeier, C., Bartling, H., Magerl, K. & Gschwind, R. M. LED-illuminated NMR studies of flavin-catalyzed photooxidations reveal solvent control of the electron-transfer mechanism. *Angew Chem Int Ed Engl* **54**, 1347–1351, doi:10.1002/anie.201409146 (2015).
14. Bartling, H., Eisenhofer, A., König, B. & Gschwind, R. M. The Photocatalyzed Aza-Henry Reaction of N-Aryltetrahydroisoquinolines: Comprehensive Mechanism, H•- versus H+-Abstraction, and Background Reactions. *Journal of the American Chemical Society* **138**, 11860–11871, doi:10.1021/jacs.6b06658 (2016).
15. Dolinski, N. D. *et al.* A Versatile Approach for In Situ Monitoring of Photoswitches and Photopolymerizations. *ChemPhotoChem* **1**, 125-131, doi:10.1002/cptc.201600045 (2017).
16. Niu, J. *et al.* Rapid Visible Light-Mediated Controlled Aqueous Polymerization with In Situ Monitoring. *ACS Macro Letters* **6**, 1109–1113, doi:10.1021/acsmacrolett.7b00587 (2017).
17. Lee, J. H. & Cavagnero, S. A novel tri-enzyme system in combination with laser-driven NMR enables efficient nuclear polarization of biomolecules in solution. *J Phys Chem B* **117**, 6069–6081, doi:10.1021/jp4010168 (2013).
18. Kuhn, L. T. Photo-CIDNP NMR spectroscopy of amino acids and proteins. *Top Curr Chem* **338**, 229–300, doi:10.1007/128_2013_427 (2013).
19. Mompean, M. *et al.* Pushing nuclear magnetic resonance sensitivity limits with microfluidics and photo-chemically induced dynamic nuclear polarization. *Nat Commun* **9**, 108, doi:10.1038/s41467-017-02575-0 (2018).
20. Okuno, Y. *et al.* Laser- and cryogenic probe-assisted NMR enables hypersensitive analysis of biomolecules at submicromolar concentration. *Proc Natl Acad Sci U S A* **116**, 11602–11611, doi:10.1073/pnas.1820573116 (2019).
21. Kaptein, R., Dijkstra, K. & Nicolay, K. Laser photo-CIDNP as a surface probe for proteins in solution. *Nature* **274**, 293–294, doi:10.1038/274293a0 (1978).
22. Vogel, H. J. & Sykes, B. D. Laser photo-CIDNP 1H NMR studies of lysozyme, ovalbumin, and their interactions. *Journal of Magnetic Resonance (*1969*)* **59**, 197-212, doi:10.1016/0022-2364(84)90165-3 (1984).

23. Broadhurst, R. W., Dobson, C. M., Hore, P. J., Radford, S. E. & Rees, M. L. A photochemically induced dynamic nuclear polarization study of denatured states of lysozyme. *Biochemistry* **30**, 405–412, doi:10.1021/bi00216a015 (1991).
24. Goez, M. Elucidating organic reaction mechanisms using photo-CIDNP spectroscopy. *Top Curr Chem* **338**, 1–32, doi:10.1007/128_2012_348 (2013).
25. Torres, O. *et al.* Photochemical pump and NMR probe: chemically created NMR coherence on a microsecond time scale. *J Am Chem Soc* **136**, 10124–10131, doi:10.1021/ja504732u (2014).
26. Stadler, E., Dommaschk, M., Fruhwirt, P., Herges, R. & Gescheidt, G. Speeding up NMR by in Situ Photo-Induced Reversible Acceleration of T1 -Relaxation (PIRAT). *Chemphyschem* **19**, 571–574, doi:10.1002/cphc.201701304 (2018).
27. Sobol, A., Torres, F., Aicher, A., Renn, A. & Riek, R. Atto Thio 12 as a promising dye for photo-CIDNP. *J Chem Phys* **151**, 234201, doi:10.1063/1.5128575 (2019).
28. Kuprov, I. & Hore, P. J. Uniform illumination of optically dense NMR samples. *J Magn Reson* **171**, 171–175, doi:10.1016/j.jmr.2004.08.017 (2004).
29. Feldmeier, C., Bartling, H., Riedle, E. & Gschwind, R. M. LED based NMR illumination device for mechanistic studies on photochemical reactions–versatile and simple, yet surprisingly powerful. *J Magn Reson* **232**, 39–44, doi:10.1016/j.jmr.2013.04.011 (2013).
30. Lehnherr, D. *et al.* Discovery of a Photoinduced Dark Catalytic Cycle Using in Situ LED-NMR Spectroscopy. *J Am Chem Soc* **140**, 13843–13853, doi:10.1021/jacs.8b08596 (2018).
31. Bernarding, J. *et al.* Low-cost LED-based Photo-CIDNP Enables Biocompatible Hyperpolarization of (19) F for NMR and MRI at 7 T and 4.7 T. *Chemphyschem* **19**, 2453–2456, doi:10.1002/cphc.201800570 (2018).
32. Yang, H., Hofstetter, H. & Cavagnero, S. Fast-pulsing LED-enhanced NMR: A convenient and inexpensive approach to increase NMR sensitivity. *J Chem Phys* **151**, 245102, doi:10.1063/1.5131452 (2019).
33. Paululat, T., Rabe, M. & Berdnikova, D. V. Modification of an NMR probe for monitoring of photoreactions. *J Magn Reson* **327**, 106990, doi:10.1016/j.jmr.2021.106990 (2021).
34. ICH. *Stability testing: Photostability testing of new drug substances and products Q1B*, <https://database.ich.org/sites/default/files/Q1B%20Guideline.pdf> (1996).
35. Aman, W. & Thoma, K. ICH guideline for photostability testing: aspects and directions for use. *Pharmazie* **58**, 877–880 (2003).
36. Kuprov, I., Craggs, T. D., Jackson, S. E. & Hore, P. J. Spin relaxation effects in photochemically induced dynamic nuclear polarization spectroscopy of nuclei with strongly anisotropic hyperfine couplings. *J Am Chem Soc* **129**, 9004–9013, doi:10.1021/ja0705792 (2007).
37. Cabre, G. *et al.* Rationally designed azobenzene photoswitches for efficient two-photon neuronal excitation. *Nat Commun* **10**, 907, doi:10.1038/s41467-019-08796-9 (2019).

38. Tait, K. M., Parkinson, J. A., Bates, S. P., Ebenezer, W. J. & Jones, A. C. The novel use of NMR spectroscopy with in situ laser irradiation to study azo photoisomerisation. *Journal of Photochemistry and Photobiology A: Chemistry* **154**, 179–188, doi:10.1016/s1010-6030(02)00347-7 (2003).
39. Wazzan, N. A., Richardson, P. R. & Jones, A. C. Cis-trans isomerisation of azobenzenes studied by laser-coupled NMR spectroscopy and DFT calculations. *Photochem Photobiol Sci* **9**, 968–974, doi:10.1039/c0pp00056f (2010).
40. Nagashima, T., Ueda, K., Nishimura, C. & Yamazaki, T. Structure-Correlation NMR Spectroscopy for Macromolecules Using Repeated Bidirectional Photoisomerization of Azobenzene. *Anal Chem* **87**, 11544–11552, doi:10.1021/acs.analchem.5b03427 (2015).
41. Stadler, E. *et al.* In Situ Observation of Photoswitching by NMR Spectroscopy: A Photochemical Analogue to the Exchange Spectroscopy Experiment. *Anal Chem* **91**, 11367–11373, doi:10.1021/acs.analchem.9b02613 (2019).
42. Seegerer, A., Nitschke, P. & Gschwind, R. M. Combined In Situ Illumination-NMR-UV/Vis Spectroscopy: A New Mechanistic Tool in Photochemistry. *Angew Chem Int Ed Engl* **57**, 7493–7497, doi:10.1002/anie.201801250 (2018).
43. Moniruzzaman, M., Talbot, J. D. R., Sabey, C. J. & Fernando, G. F. The use of1H NMR and UV–vis measurements for quantitative determination of trans/cis isomerization of a photo-responsive monomer and its copolymer. *Journal of Applied Polymer Science* **100**, 1103–1112, doi:10.1002/app.23490 (2006).
44. Nagasawa, Y. & Hirano, A. A Review of AlGaN-Based Deep-Ultraviolet Light-Emitting Diodes on Sapphire. *Applied Sciences* **8**, doi:10.3390/app8081264 (2018).

Figures

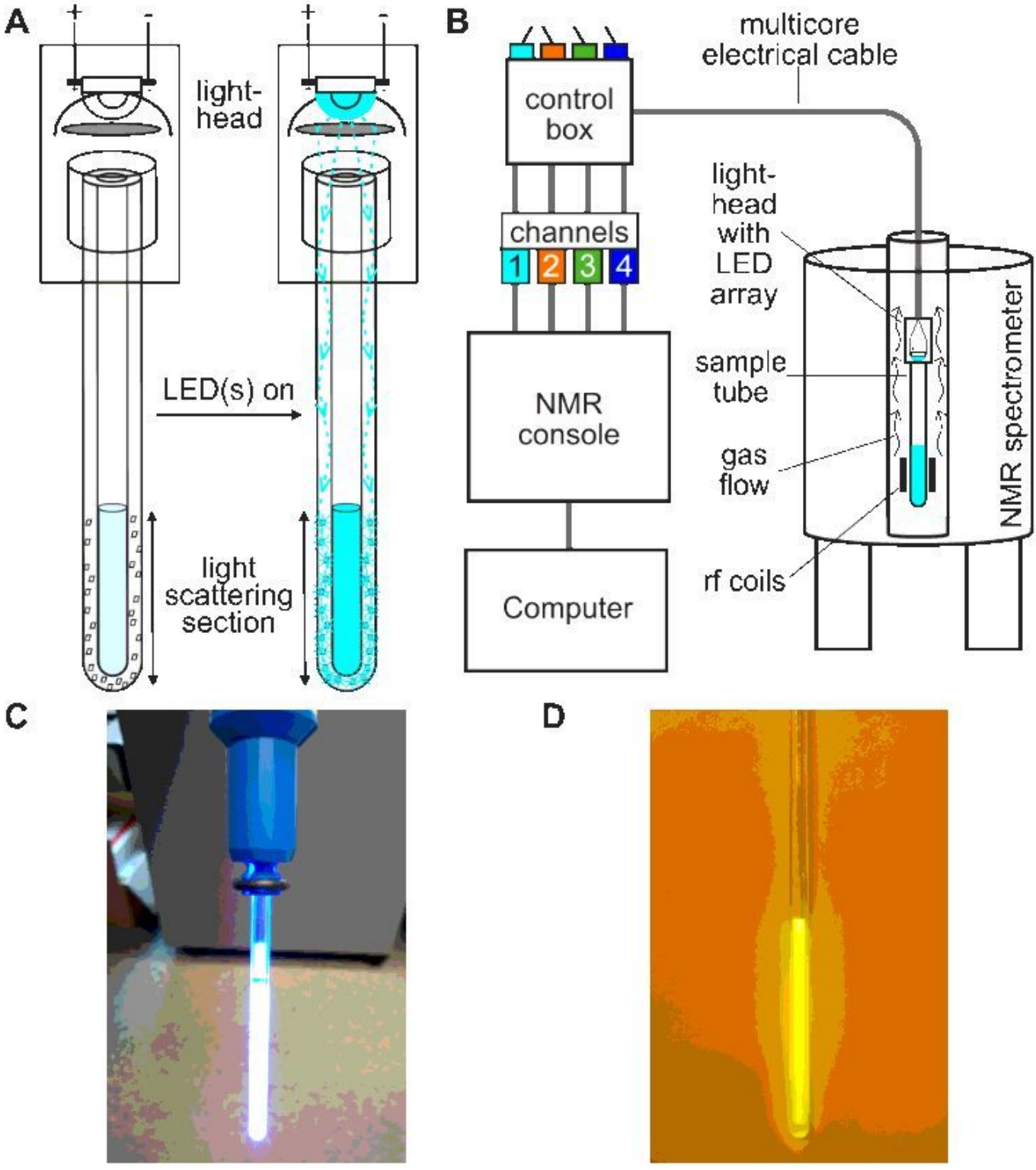

Figure 1

Principles of the NMRtorch. (A) Principle of the NMRtorch approach, with the NMR sample tube acting as a light guide. (B) Schematic of the NMRtorch setup. Not to scale. (C) Appearance under ambient light on an example NMRtorch tube filled with a typical sample and illuminated with 3W 470 nm blue LED. Scattered light appears as white due to oversaturation of the photoimaging sensor. (D) Image of

saturated solution of fluorescein sample illuminated by blue light, taken under ambient light through orange filter. The vibrant yellow fluorescence is visibly uniform across the sample.

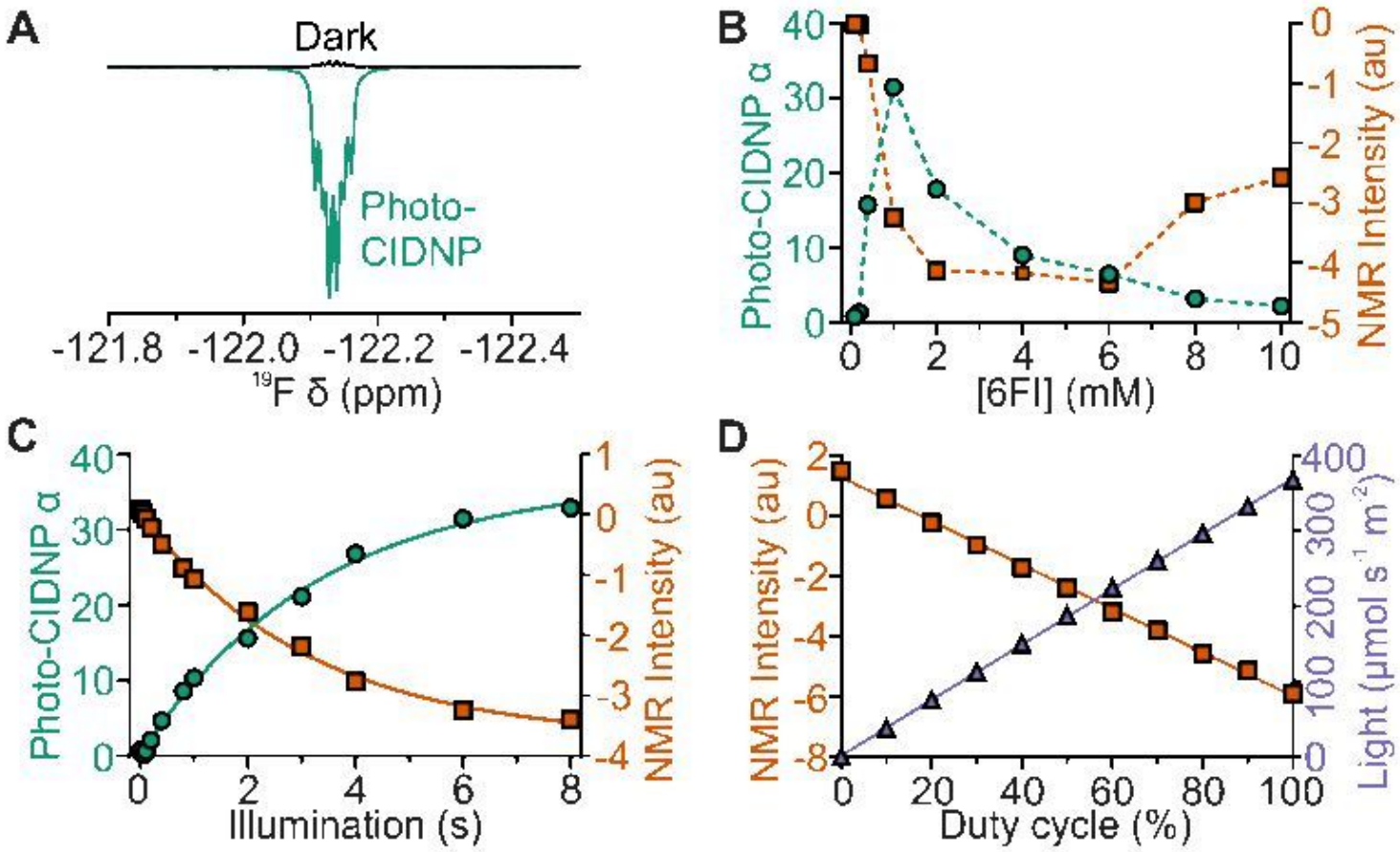

Figure 2

Photo-CIDNP effect observed for 6FI molecule using the NMRtorch apparatus. (A) Maximum observed 6FI photo-CIDNP effect, with 1 mM 6FI and 0.4 mM FMN, following 6 s illumination with 470 nm light. Both dark and illuminated photo-CIDNP spectra were acquired with one scan, and are shown here overlaid. (B) Effect of 6FI concentration (in the presence of 0.2 mM FMN) on 19F NMR signal intensity and photo-CIDNP enhancement factor (α), with 6 s illumination time. (C) Effect of illumination time on photo-CIDNP of 1 mM 6FI with 0.2 mM FMN, with exponential fits. (D) Effect of LED PWM duty cycle on the relative intensity of 6FI signal (at 6 mM, with 0.2 mM FMN present) recorded with 6 s illumination time. The corresponding light intensity measured in PPFD units ex situ at the side of the sample with a light meter is also shown. The experimental data show linear dependence on duty cycle. All experiments recorded with single blue LED (470 nm, 3W).

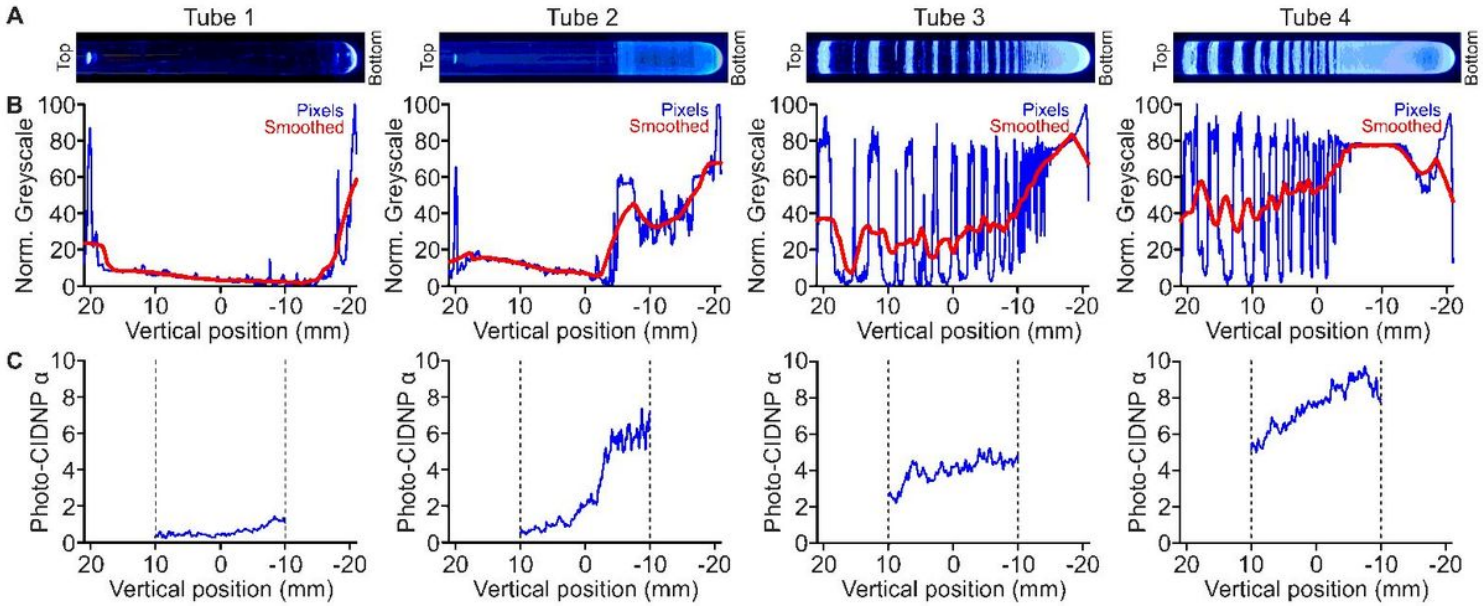

Figure 3

Effect of tube etching patterns on light distribution in NMRtorch sample tubes along the Z axis (shown here horizontally, with top of the sample on the left). Tube 1 – unetched, Tube 2 – bottom portion etched, Tubes 3 and 4 – etched in a similar pattern, with tube 4 etched more than tube 3. (A) Photo images of example tubes illuminated with attenuated 470 nm light to avoid detector saturation. (B) Pixel brightness analysis of tube images, with greyscale values normalised between lowest and highest values for each image. Smoothed values calculated using moving averages over ± 2.5 mm. The tubes in A and B were filled with H2O to a depth of 40 mm from tube bottom. (C) NMR assessment of light distribution based on position-dependent photo-CIDNP enhancement (αz) of 6 mM 6FI + 0.2 mM FMN in NMR imaging experiments with 6 s illumination times. Dashed vertical lines indicate the extent of the NMR-detectable volume. Vertical position measured along the Z-axis of the sample, relative to the centre of the NMR coil, with the positive numbers towards the top of the tube.

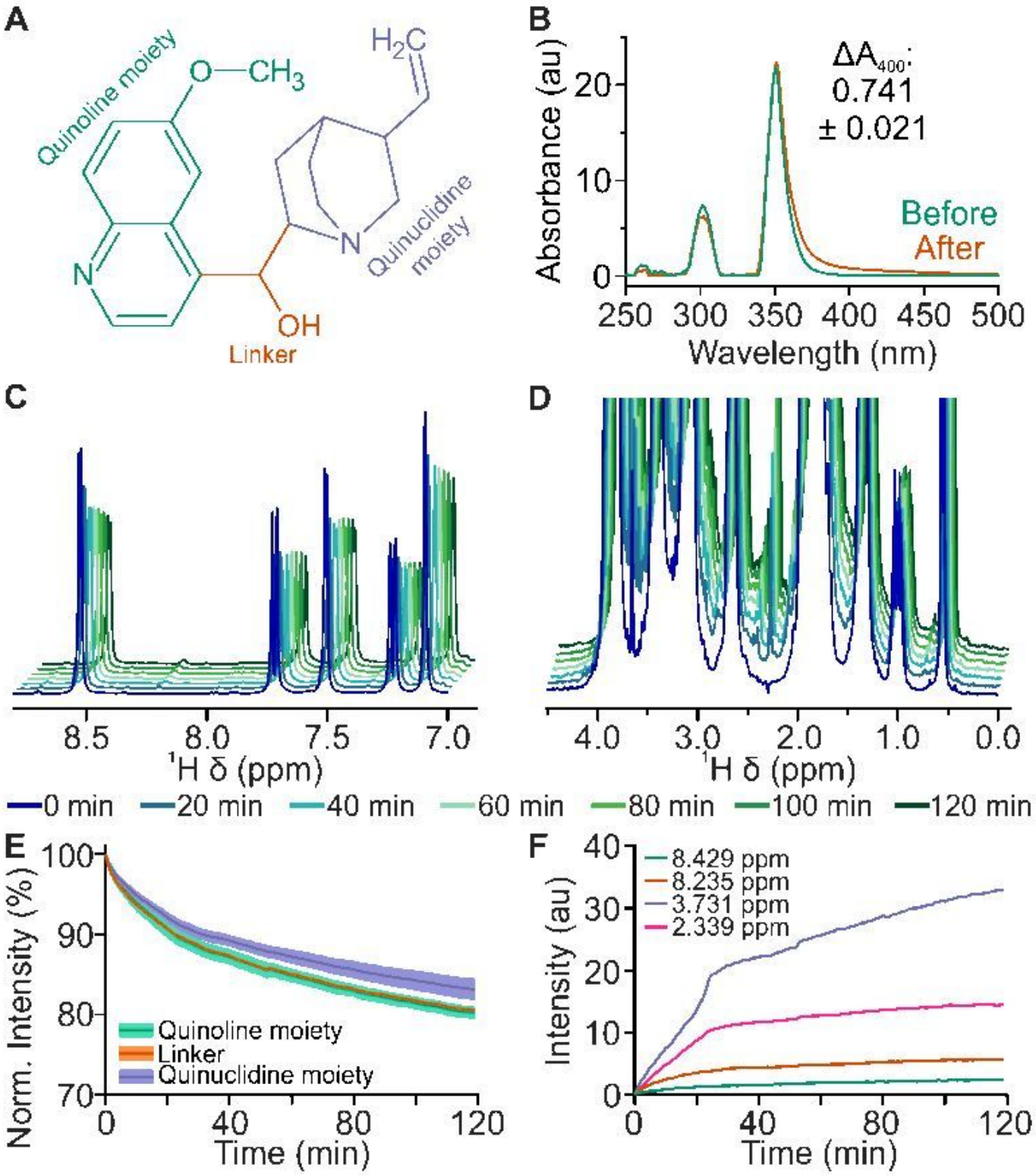

Figure 4

Photodegradation of quinine by UV irradiation using 10 W LED array with peak emission at 365 nm. (A) Chemical structure of quinine, with chemical moieties indicated. (B) UV/Vis absorbance spectrum of quinine before and after 2 hours UV irradiation in NMRtorch tube. (C) Reduction in 1H NMR signals from quinoline moiety upon in situ UV illumination, monitored continuously. (D) Changes in aliphatic 1H NMR signals, including appearance of new peaks and spectral broadening. (E) Quinine signal intensity

reduction over time, with each signal normalised against initial value. (F) Growth of degradation product signals over time.

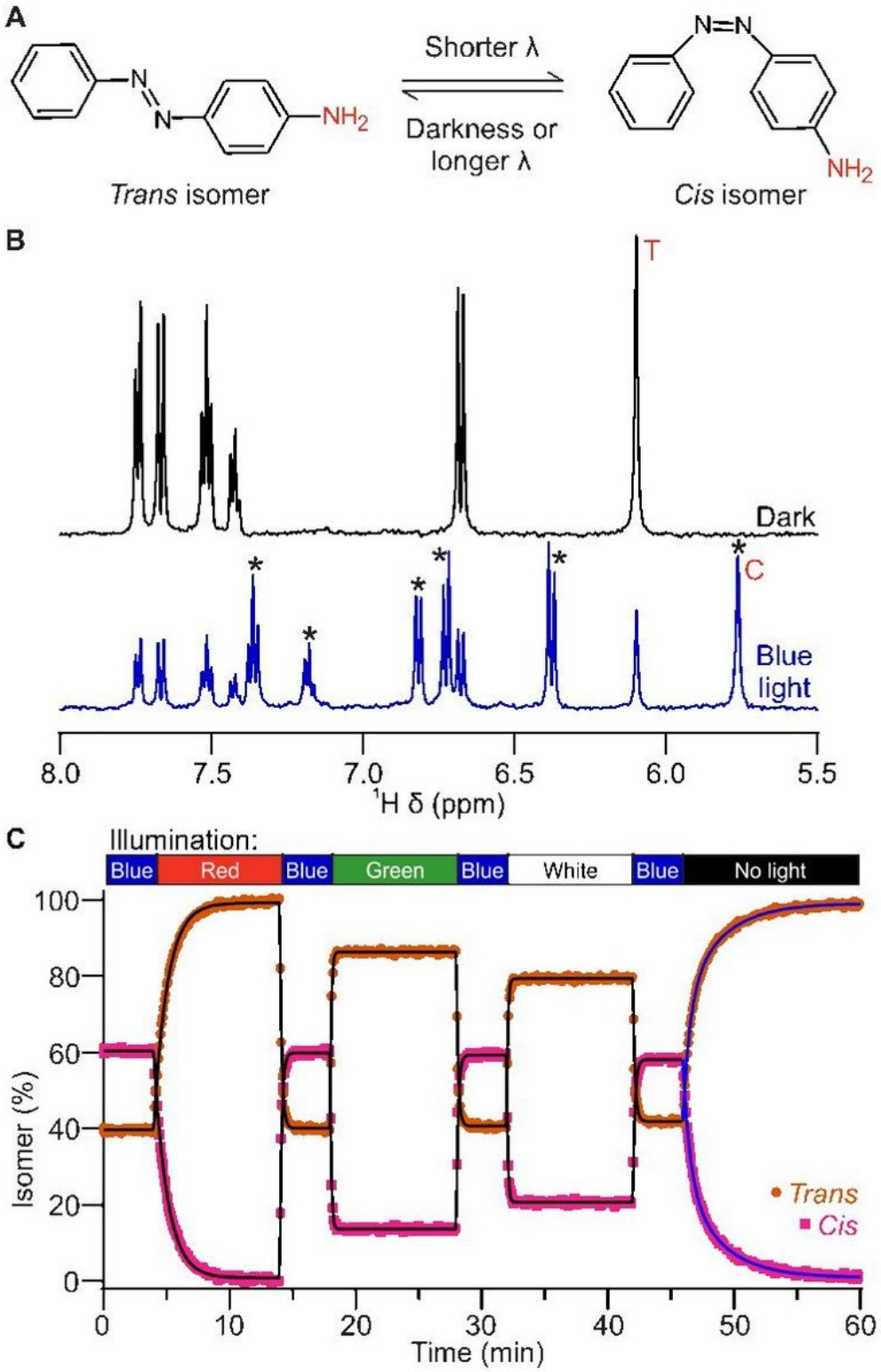

Figure 5

Photoisomerisation of 4-aminoazobenzene (AAB) studied using NMRtorch setup. (A) Schematic of trans-cis isomerisation of AAB, with amine groups used for NMR isomer assessments highlighted (red). (B) Example 1H NMR spectra at equilibrium under darkness (top) and blue light (bottom). Under darkness all

signals arise from trans isomer, while asterisks denote upfield signals arising from cis isomer appearing under blue light. Intensity of equivalent amine NMR signals marked with T (trans isomer, ~ 6.10 ppm) and C (cis isomer, ~5.76 ppm) used to determine isomer percentage. (C) Kinetics of AAB photoisomerisation studied by photo-NMR spectroscopy, with sample pre-equilibrated with blue light for 5 min before recording, and different colours toggled as indicated. The experimental data was fitted to mono- (black lines) and bi-exponential (blue lines) equations to extract kinetic parameters for individual transitions.

Supplementary Files

This is a list of supplementary files associated with this preprint. Click to download.

- SINMRtorchpaper301121.pdf